DESIGN FEATURES OF A FLAT-PLATE EXPERIMENT FOR BOUNDARY LAYER STUDIES

R.M. WATT
Dept. of Engineering Science,
University of Oxford.

ABSTRACT

Ceramic thermal barrier coatings (TBCs) are finding increasing use for thermal protection of gas-turbine hot parts. Unfortunately, TBC can result in an inferior surface finish which can have a detrimental effect on component aerodynamics.

Two-dimensional cascade tests conducted earlier highlighted the need for a detailed investigation of the effects of TBC roughness on boundary layer development. A fundamental flat-plate experiment has since been designed for the study of TBC effects on transition and turbulent boundary layers at engine-representative Mach and Reynolds numbers.

The design principles and practical features of the experiment are discussed, and selected results are presented to demonstrate the measuring techniques involved. Measurements to date apply mainly to the case of a smooth test surface used to validate the experiment against established 'base-line' data.

Presented at the 9th Turbomachinery Measuring Techniques Symposium
St Catherine's College, Oxford - March 1988.

INTRODUCTION

There is growing interest in the use of ceramic coatings for thermal protection of gas-turbine hot parts which are cooled internally. Plasma-sprayed zirconia-based coatings have low thermal conductivity, are light in weight, and are becoming increasingly resistant to high temperatures and thermal cycle fatigue. Thermal barrier coatings (TBCs) offer the potential, therefore, of economic engine life at higher operating temperatures which also has concomitant benefits in terms of engine performance.

A potential disadvantage, however, is that the coating will result in an inferior surface finish which can have a deleterious effect aerodynamically, particularly at high Reynolds numbers. Under these conditions coating roughness can promote early laminar-turbulent transition and, for fully turbulent boundary layers, increased skin-friction. The average roughness of plasma-sprayed TBC is as much as ten times that of a polished production finish, so that some influence might be expected for high-pressure first-stage aerofoils in particular.

Tests were conducted at Oxford in 1985 to determine the gross effect of TBC roughness on two-dimensional cascade efficiency [1]. These were based on the mid-height section of an advanced high-pressure nozzle-guide-vane which uses TBC to protect against turbine entry temperatures of over 2000K.

Due to the significance of the cascade test results a deeper understanding was sought of the role of TBC roughness in terms of its effects on transition and turbulent boundary layer development. A fundamental flat-plate experiment was thus proposed in which the aerodynamic effects of TBC roughness could be investigated free from surface curvature or pressure gradient effects.

The vehicle chosen for this work was the Oxford Blowdown tunnel due to its wide Reynolds number range; roughness effects being largely Reynolds number dependent. This entailed significant modifications since the Blowdown facility is normally used for cascade testing and previously had no boundary layer bleed.

DESIGN PRINCIPLES

The design of the flat-plate experiment was influenced by the following main considerations.

Firstly, the dependence of roughness effects on Reynolds number suggested the use of the Blowdown tunnel with its capacity for Reynolds number variation independent of Mach number and over a suitably wide range. In this case the Reynolds number length scale, i.e. the average roughness height, was not negotiable since TBC roughness was expected to be difficult to simulate and scale upwards due to its complex pattern (see [1]).

A basic requirement was to obtain a two-dimensional, equilibrium boundary layer originating unperturbed from the plate leading-edge. In addition, a low level of natural free-stream turbulence was required, and conversely, a means of generating turbulence (isotropic and homogeneous). To these ends the properties of 'honeycomb' flow straighteners, fine mesh screens, and inlet contractions have been considered, and various boundary layer bleed /

Nomenclature

u	:	mean velocity	u', v', w'	:	turbulent velocities
u_a	:	mean velocity in free-stream	$\overline{u'v'}$	:	turbulent shear 'stress'
y	:	distance from wall	$\overline{u'^2}, \overline{v'^2}, \overline{w'^2}$	:	turbulent normal 'stresses'
δ_{99}	:	99% boundary layer thickness	q^2	:	turbulent kinetic energy

leading-edge configurations have been investigated.

Screens and honeycombs

Fine mesh screens and 'honeycombs' are commonly used in wind tunnel testing to impose uniform mean conditions and to dampen velocity fluctuations upstream of the test section. These attributes are particularly important in studies of boundary layer transition since laminar boundary layer stability is affected by disturbances in the free-stream.

Honeycombs are effective for damping lateral mean velocities and large-scale motions such as swirl, provided the yaw angle is less than about 10 degrees (otherwise the cells 'stall') [2]. Lateral fluctuations are also inhibited and are said to be almost eliminated within 5 to 10 cell diameters. Excessive cell length, however, can result in the production of more turbulence than is suppressed and so for optimum benefit cell length should be 6 to 8 cell diameters.

A honeycomb-screen combination can reduce the turbulence level further. A fine mesh screen immediately downstream reduces the scale and intensity of turbulence generated by a honeycomb. The important parameter is the pressure-drop coefficient, K, which is the ratio of pressure drop to dynamic pressure, and which is a function of screen open-area ratio and Reynolds number. A value for K of around 2 gives effective attenuation of free-stream turbulence, particularly in the longitudinal or mean flow direction [2,3].

Because the local effect of screens is to cause a pressure drop proportional to velocity squared, they can also be used to make velocity profiles more uniform and to thereby reduce inlet boundary layer thickness. Screens can also help solve problems of separation at inlet.

Turbulence generation

Turbulence generated by parallel-bar or square-mesh grids becomes reasonably 'homogeneous' (invariant to axis translation) and roughly 'isotropic' (invariant to axis rotation) within about 30 to 40 mesh lengths [3]. Homogeneity and isotropy represent identifiable and reproducable standards which, although not necessarily representative of a gas-turbine environment, are generally desirable in a research context.

Axial contractions are often used to improve the isotropy of grid-generated turbulence. Without any remedial action, at 30 to 40 mesh lengths the longitudinal component of turbulence (rms) exceeds that of the lateral components in the approximate ratio of 1.15 : 1. From [3], a contraction ratio of 1.3:1 will reduce this ratio to almost unity. Axial contractions act to amplify lateral fluctuations and dampen longitudinal ones.

Axial contractions need to be carefully designed to avoid the possibility of a surface velocity 'overshoot', since during recovery from this the associated positive, or 'adverse', pressure gradient might precipitate separation [4,5]. In qualitative terms it could be said that the profiles in the contraction transition zones require to be extremely smooth and gradual. More precise criteria are provided in [5] on which an in-house routine for the design of 'separation-free' contractions is based.

Correlations for the decay of turbulence intensity behind a grid may be found in the literature [6,7]. These depend on the grid geometry and the distance downstream, and so for a desired level of turbulence at the test section, provide some basic design criteria for the grid. Another vital consideration is the minimum grid solidity which will cause 'choking'.

Boundary-layer bleed and leading-edge configuration

In transition studies it is crucial to avoid a separation at the plate leading edge as this will almost certainly 'trip' the boundary layer, causing it to go turbulent. Leading-edge shapes are often elliptical precisely to prevent a separation and premature transition. The flat-plate test section described in [8], for instance, has a 4:1 elliptical leading-edge which appears to be typical.

References [9,10] refer to the control provided by varying plate incidence. In these cases, with the plate mounted in the free-stream, a slight positive incidence of approximately 0.5 degrees was sufficient to avoid a separation by ensuring that the stagnation point was located on the upper surface. Also noted in [9] is that the transition Reynolds number can be greatly influenced by the leading-edge shape. In general, for a 'blunt' leading-edge, transition Reynolds number is shown to vary with free-stream velocity. It is unclear whether 'bluntness' can be precisely defined in this situation.

The main requirements of the boundary layer bleed are to have the capacity to remove the boundary layer mass flow with some in reserve at all conditions, and to maintain this bleed constant for a period compatible with the run-time of the tunnel, i.e. approximately 2 secs. *A priori*, the mass flow in the boundary layer may be estimated from predictions of the velocity profile or the boundary layer thickness parameters. It must be ensured that the effective throat area of the bleed pipework is more than sufficient to cope with this without 'choking'. If, as in this case, the bleed is connected to a dump tank this must be of sufficient volume to sustain a constant flow rate for the required time. Specific details of the present arrangement are given below.

EXPERIMENTAL APPARATUS

A photograph of the experiment *in situ* is shown in Figure 1. The Blowdown tank, which is shown open for access, is normally closed forming a plenum chamber containing the working section. The flat-plate experiment is shown secured to a wedge-shaped base in place of the usual two-dimensional cascade. Other noticeable features are a measuring microscope which is removed before each run, and the near-side leg of the boundary layer bleed pipework.

Working section

A sectional drawing of the working section is shown in Figure 2. The inlet profile is elliptical, leading to a constant-area section followed by a 1.3:1 contraction to improve the isotropy of grid-generated turbulence. A honeycomb of cell-length to diameter ratio of approximately 8 is installed to 'straighten' the inlet flow and to reduce the free-stream turbulence. Fine mesh screens are installed either side of the honeycomb to further reduce the turbulence level. The calculated screen pressure drop coefficient at a typical test Reynolds number is approximately 1.0, which, according to [3], should attenuate u' by about 80% and v' by about 40%.

When more than the minimum free-stream turbulence is desired a square-mesh turbulence grid (a perforated plate) is fitted. Its axial position can be adjusted to control the intensity of turbulence at the test section. At least 30 to 40 mesh lengths are allowed to ensure reasonable homogeneity before the start of the 1.3:1 contraction. The contraction was designed using the method of [5] which, for a given contraction ratio and length, calculates a cubical-arc profile for the avoidance of excessive low pressures and hence unfavourable pressure gradients

which might precipitate separation.

The flat-plate test piece is detachable and can move axially back or forth. It is 0.3m long and 0.2m wide, and the test section width to height ratio is two. As shown, the final leading-edge shape is that of a 'knife-edge' although various other profiles were investigated. The opposite wall can be inclined to vary streamwise pressure gradient if desired or to compensate for boundary layer growth. Mounting the test plate in the free-stream was not considered viable in this case mainly to do with the measuring techniques employed.

High-quality glass windows are fitted, permitting the full length of the test section to be viewed for Schlieren photography.

Boundary-layer bleed

The inlet boundary layer mass flow was estimated from computer predictions of the boundary layer thickness parameters. The minimum bleed throat area could then be estimated and also the required dump tank capacity. The rate of dump tank pressure rise and hence the mass flow rate were in fact monitored during each run.

Referring to Figure 2 , the boundary layer bleed opening is adjustable by moving the flat-plate test piece axially. The bleed opening leads to a bleed 'cell' from where the mass flow is removed on both sides of the working section. This arrangement was determined largely by spatial constraints due, in part, to the existence of mechanisms underneath the test section. The two-dimensionality of the flow into the bleed was checked using oil-dot flow visualisation.

The boundary layer bleed system is shown in diagramatic form in Figure 3. A 20 ft^3 capacity dump tank is evacuated prior to the run by means of a rotary-piston vacuum pump (displacement 35 ft^3/min). The line is opened to dump tank pressure by the action of an electro-pneumatic ball valve, whose timing is controlled inside the Blowdown cabin, and the mass flow rate is controlled by a manually adjusted gate valve. Almost all of the hardware shown in Figure 3 is new to the Blowdown tunnel.

MEASURING TECHNIQUES

Schlieren photography was used to indicate the state of the flat-plate boundary layer and also conditions in the vicinity of the boundary layer bleed and leading edge. Being sensitive to density gradient, the Schlieren technique provides at least a useful qualitative picture of the flow field. In this application the equipment was configured to reveal density gradients in the cross-stream direction, i.e. vertically across the boundary layer.

The study of boundary layers developing on TBC flat-plate surfaces involves the measurement of boundary layer profiles at a number of streamwise stations. When various operating conditions are also envisaged the test-programme matrix can become prohibitive, particularly when the wind tunnel facility is of the intermittent type and the 'turn-round' time is not insignificant. For this reason it was decided to make use of the existing motorised traverse mechanism for 'dynamic' boundary layer traversing in order to accomplish one traverse per run.

The existing four-axis traverse mechanism is situated on the floor of the working section below the flat-plate test piece. It is controlled by dedicated microprocessors and is normally used in cascade testing to traverse pressure probes past wakes. A special traverse attachment was made to accept hot-wire or pitot probes and the traverse was programmed to move these vertically through the boundary layer. The special

attachment permits the probe minimum height to be set thereby protecting the probe tip from surface contact.

Boundary layer mean velocity profiles were measured conventionally using an 'impact' or total pressure probe. Although this technique has been used previously in the OUEL Blowdown tunnel, the present arrangement was specially designed for improved frequency response. This was important even for the measurement of mean quantities because of the intention to traverse dynamically. Whereas previously the probe was physically remote from the pressure transducer - the two being connected by a short length of pneumatic tubing - the present 'fast-response' probe actually embodies the transducer as shown in Figure 4. The 'ultraminiature' pressure transducer (KULITE CQ-030) fits into the bore of the pitot probe to approximately 25mm from the flattened tip.

Hot-wire anemometry has a major role in the experiment for the measurement of turbulence quantities such as three-component velocity fluctuations and turbulent or Reynolds stresses. In addition the fluctuating output from hot-wires is also a sensitive indicator of boundary layer transition. Both single-sensor and dual-sensor (x-array) hot-wire probes have been employed for these purposes as well as hot-film probes which were considered partly for their robustness. Although the measuring probes could be traversed vertically as described earlier, all hot-wire measurements of the boundary layer turbulence quantities were made at fixed heights to obtain representative time samples at each height.

The two main types of probe used are illustrated in Figure 5. All were used in conjunction with one or two DISA 'M-series' main units operating in constant temperature mode.

The measuring microscope shown in Figure 1 was used to determine the distance between the pitot or hot-wire probes and the surface prior to each run. Its vertical position can be resolved to within 0.02mm using an incorporated vernier scale, and by this means the hot-wire probe tip could be safely taken to within 0.25mm from the surface. A 'goniometer' or protractor type eyepiece was fitted to measure the incidence angles of crossed hot-wires. The measuring microscope runs freely on a grooved sideplate which is also graduated to indicate the axial or streamwise position of the probe.

Finally, the then novel technique described in [1], of transition detection using surface thin film gauges painted and fired onto TBC surfaces, will be employed again in this experiment and will be reported at a later date.

SELECTED RESULTS

Before proceeding to study roughness effects it is important to evaluate the experimental set-up (rig and instrumentation) for the simpler case of a test surface which is smooth. Selected results from this are described below.

Initially, checks were made of the performance of the inlet design and of the boundary layer bleed system. Oil-dot visualisation was used to look for signs of flow irregularities along the inlet profile and to check the two-dimensionality of the flow into the bleed. A 100-point pressure survey was made at the contraction exit plane to prove that the core-flow total pressure was sufficiently uniform.

Using a single-sensor hot-wire, the natural level of free-stream turbulence at the test-section without honeycomb flow straighteners or fine mesh screens measured approximately 1.3%. This was reduced to a more acceptable level of approximately 0.75%, using the honeycomb-screen combination described

earlier. With the turbulence grid in place and using an x-array hot-wire probe the measured free-stream turbulence was approximately 3.7%, which was acceptably close to the design base level, grid-in, of 4%. The turbulence isotropy was measured by rotating the x-array probe through 90 degrees and was found to be acceptable within the repeatability of the measurements.

Significant changes were required to the plate leading-edge arrangement to avoid tripping the boundary layer; various leading-edge ellipticities and thicknesses were tried and the height and axial position of the flat plate were varied in relation to the adjacent inlet. The final, successful configuration was that of a 'knife-edge' with the plate flush with the inlet.

Schlieren photographs taken at different conditions are shown in Figure 6. These clearly show the flat-plate boundary layers and also flow conditions in the vicinity of the boundary layer bleed. In Fig. 6(a), the smooth-wall datum case, transition is observed mid-way along the plate and the subsequent growth of the turbulent boundary layer is quite apparent. The effect of increasing free-stream turbulence intensity is as expected with transition perceptible nearer the plate leading-edge - Fig. 6(b). The turbulence in the free-stream is itself evident from this photograph. Finally, Fig. 6(c) illustrates the basic effect of roughness on transition, where, for this grade of sand-grain, transition appears to be immediate, at the plate leading-edge.

Turbulent mean velocity profiles measured using the 'fast-response' pitot probe are shown in Figure 7. This compares profiles on 'rough' (TBC) and smooth surfaces measured at the same distance from the plate leading-edge and at the same conditions. The comparison mainly reflects the effect of TBC roughness on transition and on turbulent boundary layer growth. This aside, Figure 7 is mainly intended to demonstrate the efficacy of the pitot technique.

In fact the use of the new pitot probe was not straightforward, mainly as a result of mechanical problems associated with the small scale of the transducer and due to the demands of the operating environment. For instance, the delicate wires of the transducer were prone to come loose, requiring removal of the probe and re-attachment under the microscope.

Hot-wire time histories at a number of streamwise stations and at a fixed height are shown in Figure 8. These appear to display the sporadic peaks usually associated with the growth and passage of turbulent spots, leading to higher frequency fluctuations in turbulence.

The same signals are displayed in the frequency domain in Figure 9 which gives an interesting qualitative picture of the transition process.

Based on these and other results and taking free-stream turbulence into account the Reynolds number for transition compares favourably with correlations [10].

Finally, turbulence measurements normal to the surface were made at the last streamwise station using an x-array hot-wire. For this the boundary layer bleed was disabled to provide a suitably thick boundary layer for measurement purposes. The boundary layer 'structural coefficients' are seen to compare reasonably well with established data. The x-array hot-wire signals were processed according to the procedure of [11].

CONCLUSION

A flat-plate experiment for boundary layer studies on TBC rough surfaces has been designed and tested in the Oxford Blowdown tunnel. Initial results of rig validation tests using a smooth surface appear consistent with established data.

REFERENCES

[1] R.M.Watt, N.C.Baines, J.L.Allen, J.P.Simons, M.George, " A Study of the Effects of Thermal Barrier Coating Surface Roughness on the Boundary Layer Characteristics of Gas-Turbine Aerofoils", ASME Paper No. 87-GT-223.

[2] R.D.Mehta & P.Bradshaw, " Design Rules for Small Low-Speed Wind Tunnels", Aeronautical Journal, November, 1979.

[3] S.Corrsin, "Turbulence: Experimental Methods ", article in Encyclopedia of Physics, Vol 8, Berlin, 1963.

[4] F.Cheers, " Note on Wind-Tunnel Contractions ", R & M 2137, March, 1945.

[5] H.Rouse & M.M.Hassan, "Cavitation-Free Inlets and Contractions", Mechanical Engineering, March, 1949.

[6] P.E.Roach, "The Generation of Nearly Isotropic Turbulence by Means of Grids", Int. J. Heat Fluid Flow, Vol 8, No. 2, June 1987.

[7] J.P.Gostelow, "Cascade Aerodynamics", Pergamon Press, 1984.

[8] M.F.Blair et al, "Development of a Large-Scale Wind Tunnel for the Simulation of Turbomachinery Airfoil Boundary Layers", ASME Paper No. 81-GT-6.

[9] A.A.Hall & G.S.Hislop, "Experiments on the Transition of the Laminar Boundary Layer on a Flat Plate", R & M 1843, August, 1938.

[10] B.J.Abu-Ghannam & R.Shaw, "Natural Transition of Boundary Layers - the Effects of Turbulence, Pressure Gradient and Flow History", Journal of Mechanical Engineering Science, Vol 22, 1980.

[11] F.Klatt, "The X Hot-Wire Probe in a Plane Flow Field", DISA Information No. 8, July 1969.

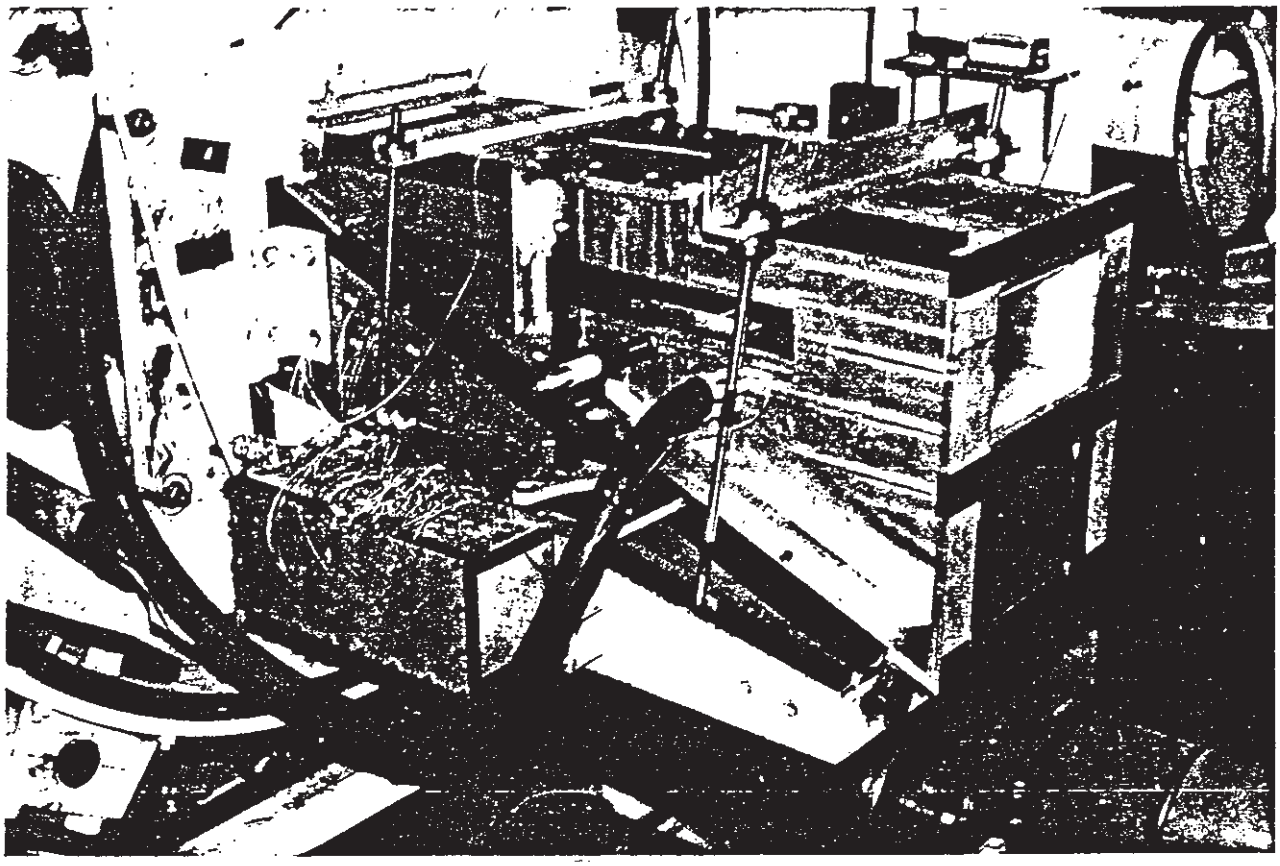

FIG 1 Photograph of the experiment in the OUEL blowdown tunnel

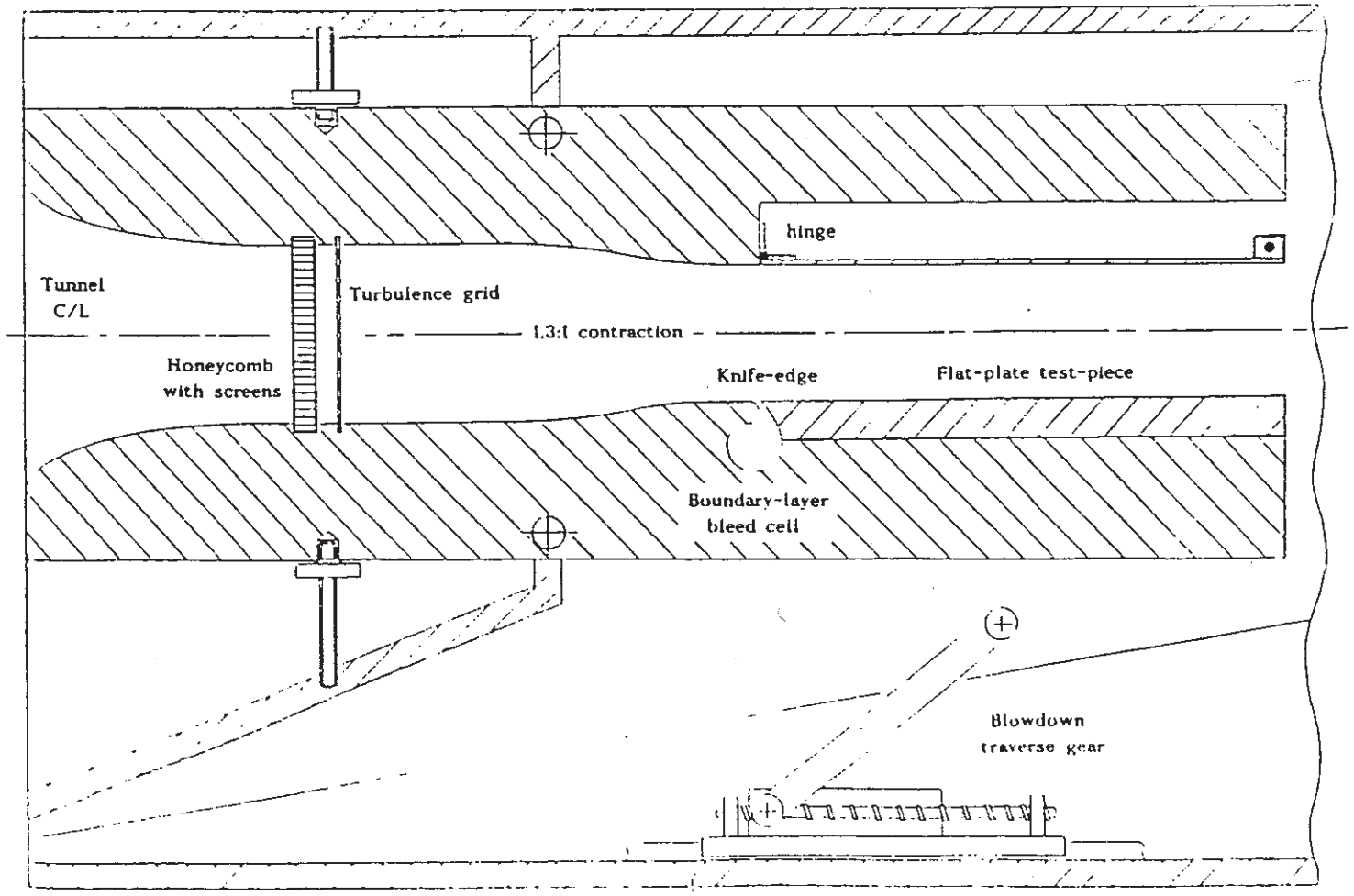

FIG 2. Sectional view of the working-section

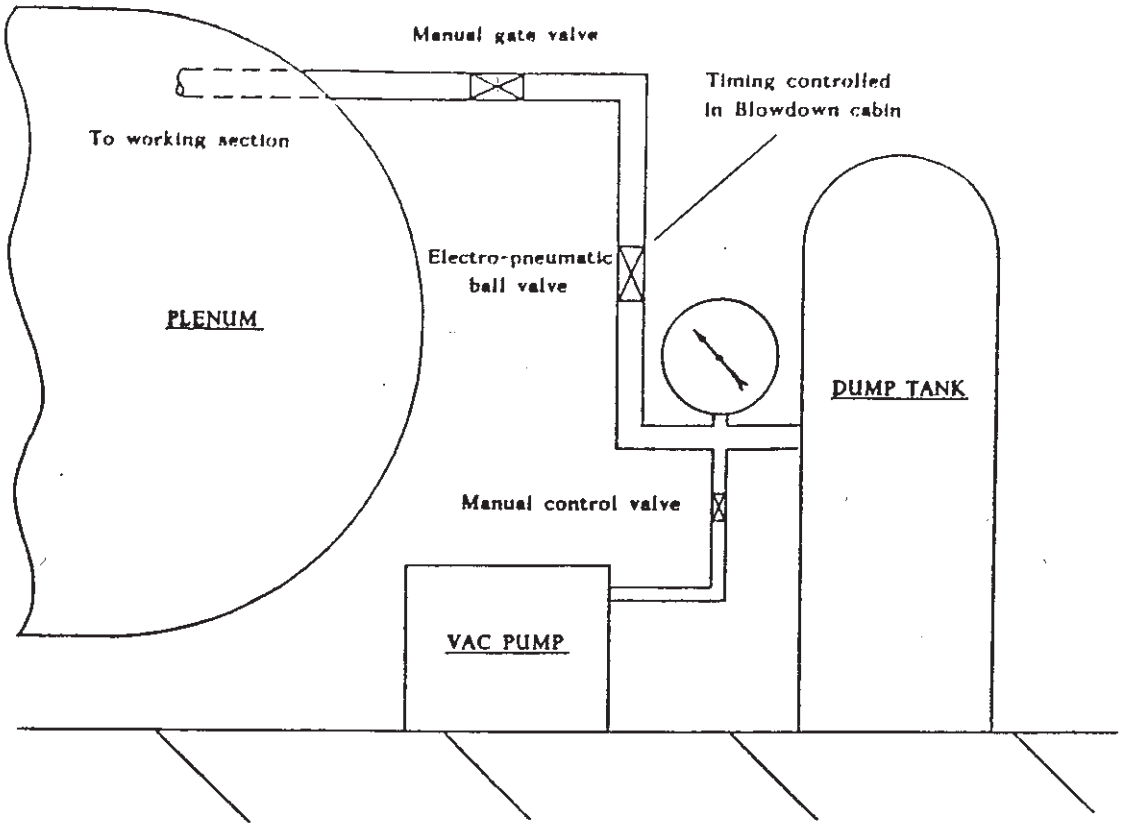

FIG 3. Schematic of the boundary layer bleed system

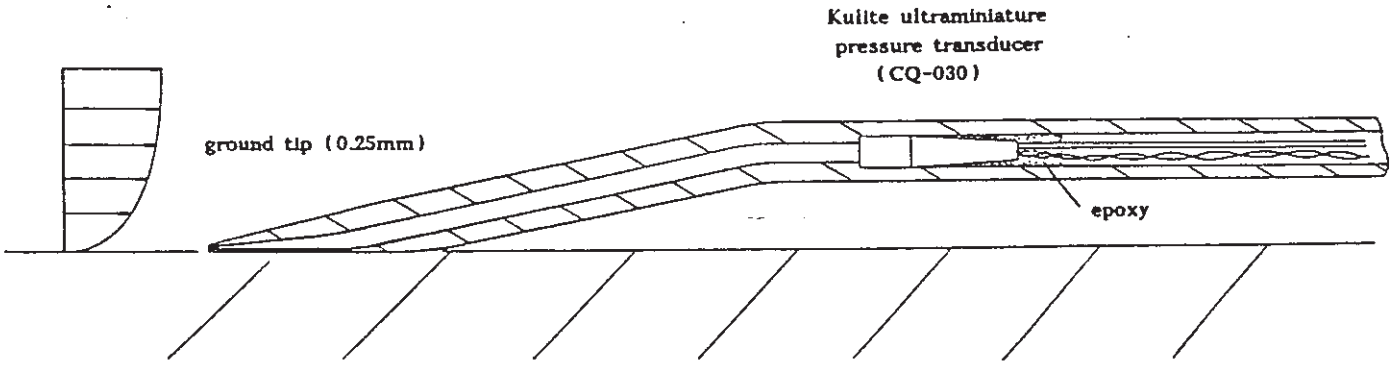

FIG 4. The 'fast-response' total-pressure probe

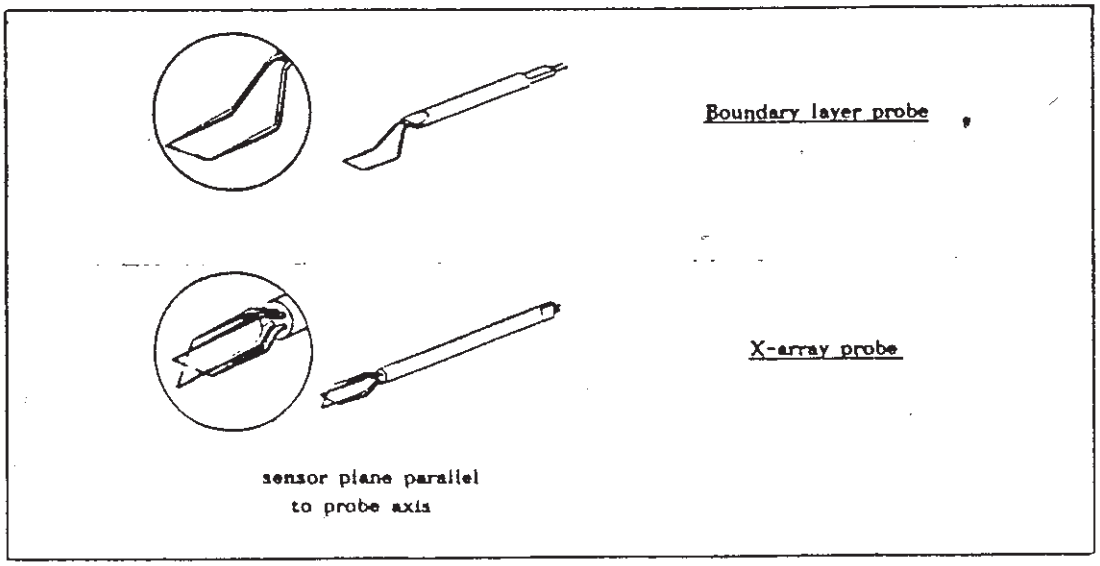

FIG 5. Hot-wire anemometry probes

(a) Smooth datum case

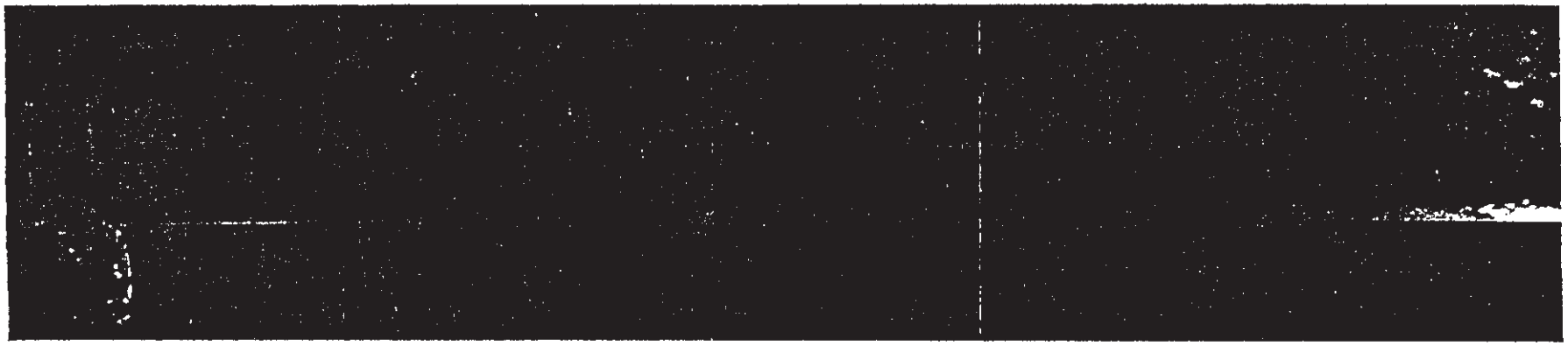

FLOW

(b) Smooth, grid-in

(c) Sand grain roughness

FIG 6. Schlieren photographs of flat-plate boundary layers

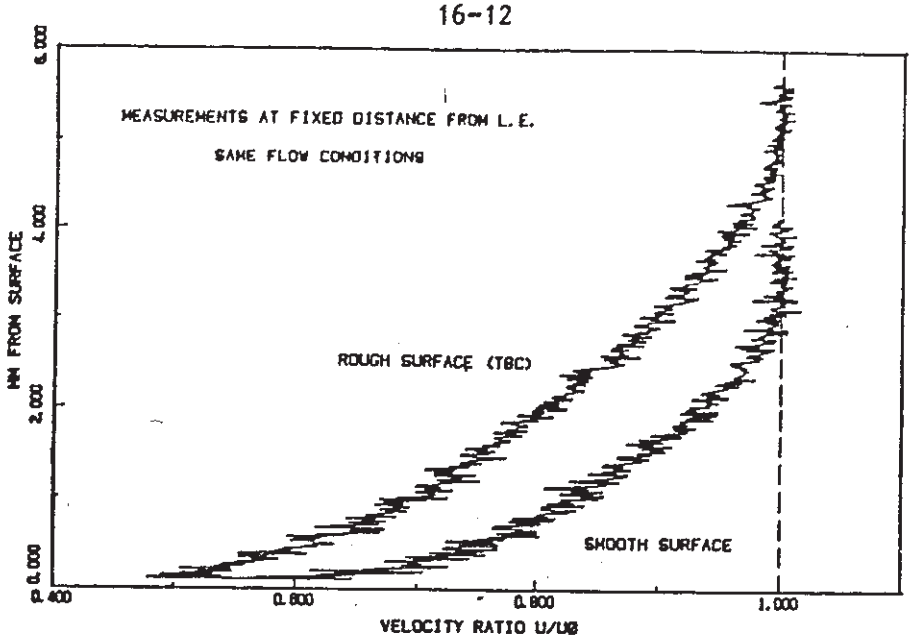

FIG 7. Turbulent velocity profiles by pitot-traverse

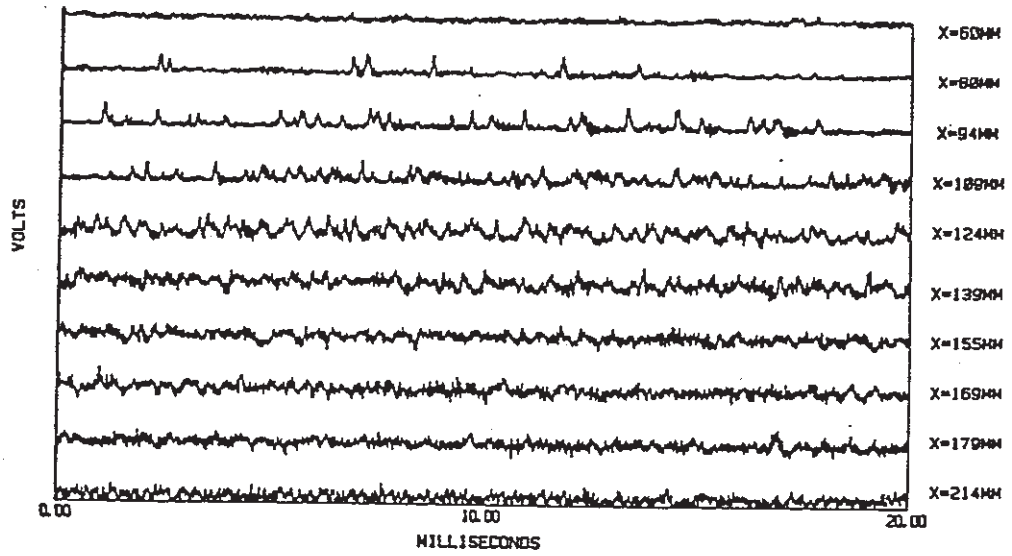

FIG 8. Hot-wire time histories showing transition

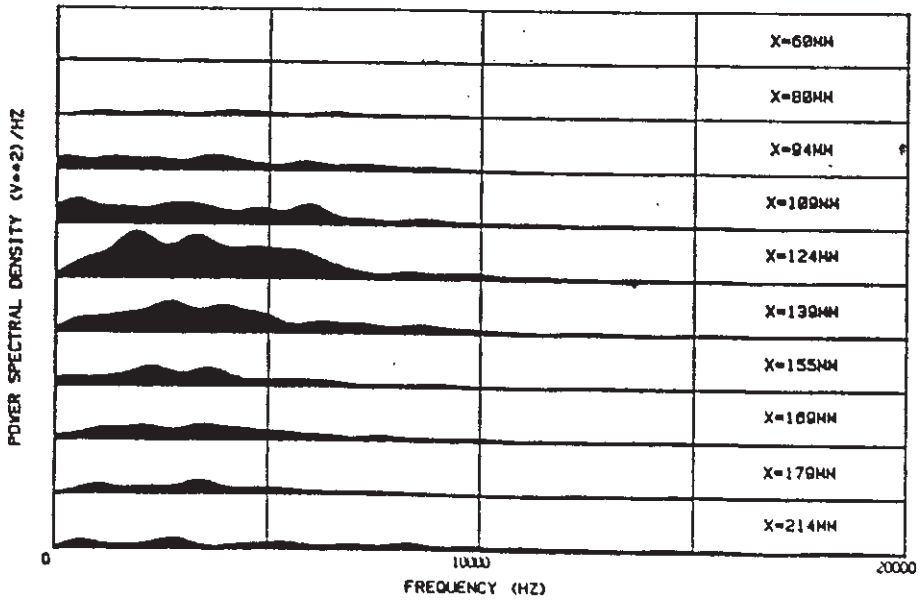

FIG 9. Hot-wire power spectra

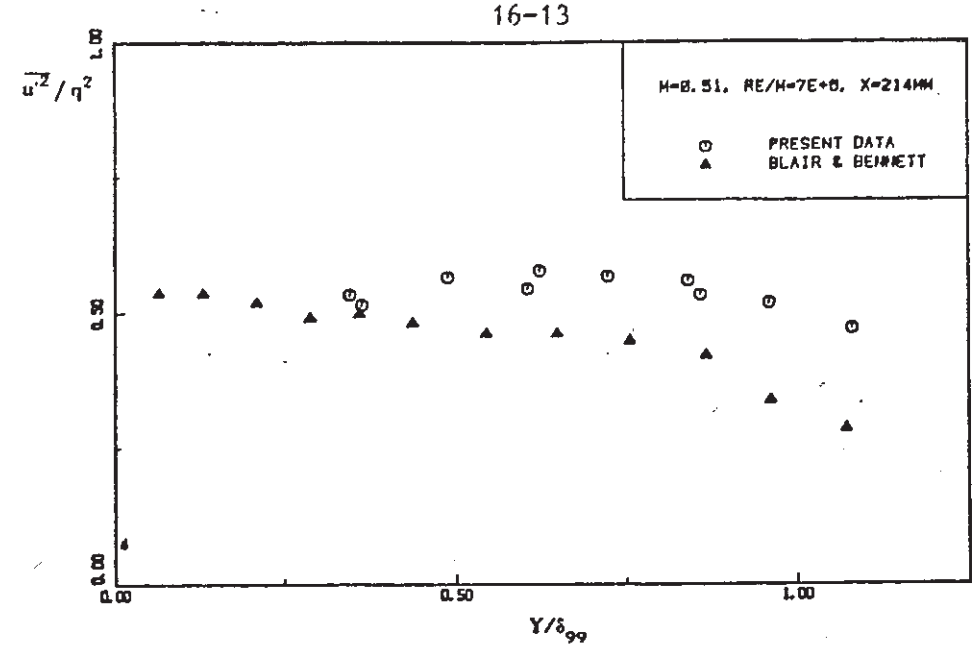

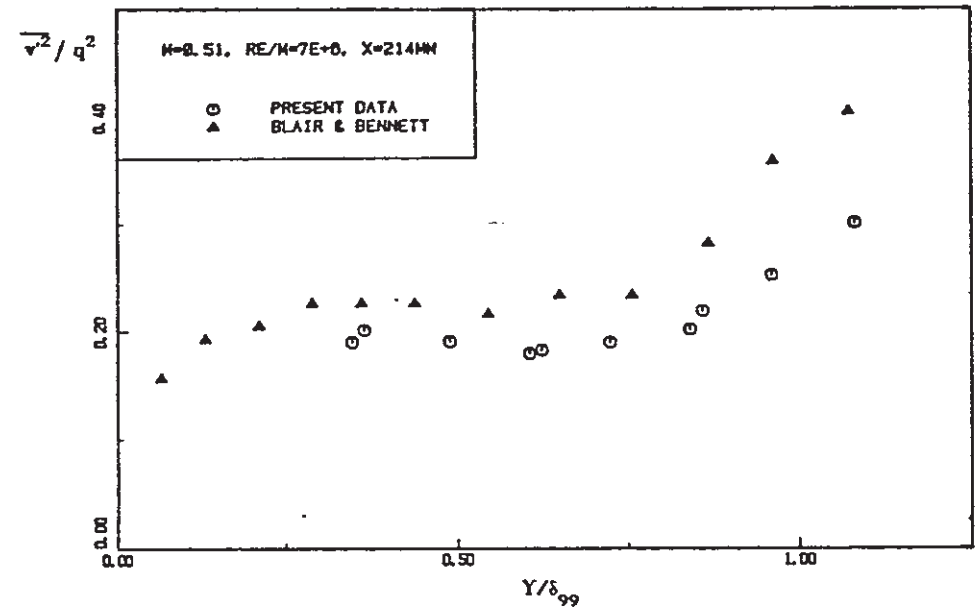

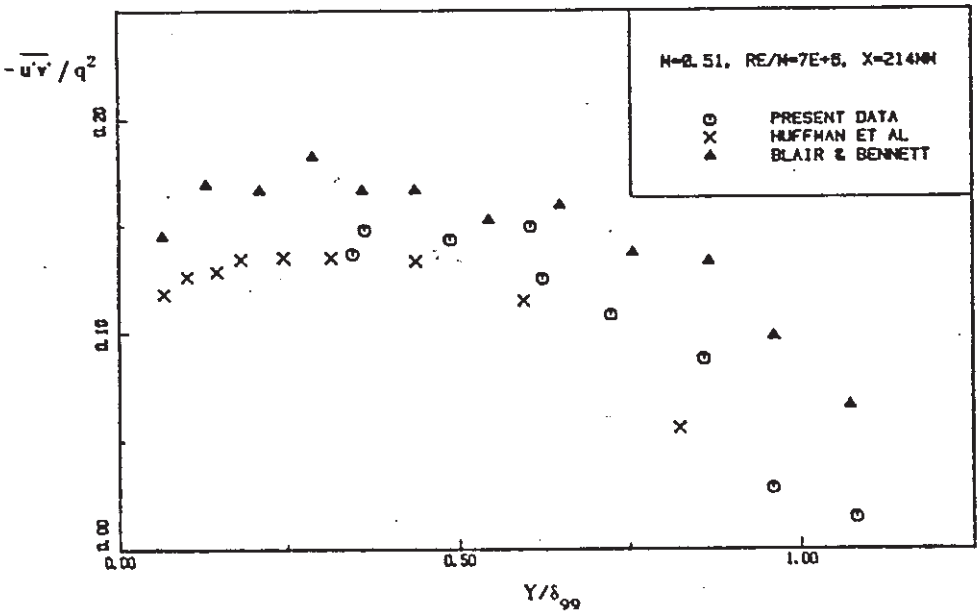

FIG 10. Boundary layer turbulence profiles